Journal of Solid Mechanics Vol. 8, No. 2 (2016) pp. 262-279

The Effect of Elastic Foundations on the Buckling Behavior of Functionally Graded Carbon Nanotube-Reinforced Composite Plates in Thermal Environments Using a Meshfree Method

Sh. Shams , B. Soltani *, M. Memar Ardestani

Faculty of Mechanical Engineering, University of Kashan, Kashan, Iran

Received 5 February 2016; accepted 26 March 2016

ABSTRACT

The buckling behavior of functionally graded carbon nanotube-reinforced composite (FG-CNTRC) plates resting on Winkler-Pasternak elastic foundations under in-plane loads for various temperatures is investigated using element-free Galerkin (EFG) method based on first-order shear deformation theory (FSDT). The modified shear correction factor is used based on energy equivalence principle. Carbon nanotubes (CNTs) are embedded in polymer matrix and distributed in four types of arrangements. The temperature-dependent material properties of an FG-CNTRC plate are assumed to be graded along the thickness direction of the plate and estimated through a micromechanical model based on the extended rule of mixture. Full transformation approach is employed to enforce essential boundary conditions. The modified shear correction factor is utilized based on energy equivalence principle involving the actual non-uniform shear stress distribution through the thickness of the FG-CNTRC plate. The accuracy and convergency of the EFG method is established by comparing the obtained results with available literature. Moreover, the effects of elastic foundation parameters are investigated for various boundary conditions, temperatures, plate width-to-thickness and aspect ratios, and CNT distributions and volume fractions. Detailed parametric studies demonstrate that the elastic foundation parameters, CNT distributions along the thickness direction of the plate and the temperature change have noticeable effects on buckling behavior of carbon nanotube-reinforced composite (CNTRC) plates.

Keywords : Buckling; Composite plate; Carbon nanotubes; Elastic foundation; Meshfree method; First-order shear deformation theory.

1 INTRODUCTION

THE supreme and outstanding characteristics of carbon nanotubes (CNTs) broadly attract researchers' attention in recent years. The extraordinary mechanical, electrical and thermal properties of CNTs make them as one of the most promising reinforcement materials for high performance structural and multifunctional composites instead of conventional fibers [1-4]. Introducing CNTs as reinforcements for polymers leaded to several important studies to estimate their mechanical properties accurately [5-9]. These studies have proved that applying small amount of CNTs to the matrix can effectively enhance overall mechanical and electrical properties of polymeric composites [7-10].In practice, this behavior makes them appropriate for aerospace applications as well as electronics and transport industries [11].

*Corresponding author. Tel.: +98 9128092210 ; Fax: +98 361 5912424.
E-mail address: bsoltani@kashanu.ac.ir (B. Soltani).

Recently, many investigations considering structural applications of carbon nanotube reinforced-composites (CNTRCs) have been done. Jafari Mehrabadi et al. [12] presented mechanical buckling of nanocomposites rectangular plate reinforced by aligned and straight single-walled carbon nanotubes (SWCNTs) based on first-order shear deformation theory (FSDT). They used both the Eshelby-Mori-Tanaka approach and the extended rule of mixture to evaluate the effective material properties of CNTs. Buckling analysis of quadrilateral laminated plates with CNTRC layers employing a mapping-differential quadrature technique is investigated by Malekzadeh and Shojaee [13]. They examined the effects of volume fraction of CNTs, geometrical parameters, thickness-to-length ratio, CNT distribution profiles and boundary conditions on the critical buckling load.

Functionally graded carbon nanotube-reinforced composites (FG-CNTRCs) are new types of nanocomposites in which the material composition is varied continuously along thickness direction according to CNT volume fractions. The material properties of FG-CNTRCs can be evaluated through a micromechanical model in which CNT efficiency parameters are estimated by matching the elastic moduli of the CNTRCs observed from the molecular dynamics (MD) simulation with that of numerical results obtained from the rule of mixture [14]. Analysis of FG-CNTRC plates were first presented by Shen [14] in which he studied the nonlinear bending behavior of FG-CNTRC plates in thermal environment. He concluded that the load-bending moment curves of the plate could be significantly increased as a result of functionally graded CNT reinforcements. Zhu et al. investigated linear bending and free vibration behaviors of FG-CNTRC plates with various distributions of reinforcements under different width-to-thickness ratios using finite element method (FEM) [15]. Sobhani Aragh et al. studies the vibration behavior of continuously graded CNTRC cylindrical panel using an equivalent continuum model based on Eshelby-Mori-Tanaka approach [16]. They demonstrated that continuously graded oriented CNT volume fractions can be used for management of vibration behavior of structures. Recently, Alibeigloo and Liew [17] presented a thermoelastic analysis of FG-CNTRC plates based on three-dimensional theory of elasticity. They investigated the effects of uniform and functionally graded distributions of CNTs, their volume fractions as well as length-to-thickness ratio of the plate. Static analysis of FG-CNTRC cylinders considering an axisymmetric model using element-free Galerkin (EFG) method was presented by Moradi-Dastjerdi et al. [18]. Large deflection analysis of FG-CNTRC plates by element-free kp-Ritz method based on von Kármán assumption was studied by Lei et al. [19]. Obtained results revealed that the change of CNT contents, plate width-to-thickness ratios and boundary conditions have pronounced effects on nonlinear responses of different types of CNTRC plates. Furthermore, buckling analysis of functionally graded carbon nanotube-reinforced composite plates using element-free kp-Ritz method was presented by Lei et. al [20]. They concluded that the distribution type of CNT significantly affects buckling strength of CNTRC plates. Nonlinear vibration of shear deformable CNTRC cylindrical panels resting on elastic foundations in thermal environments was studied by Shen and Xiang [21]. They revealed that the natural frequencies are increased by increasing the CNT volume fraction, while the CNTRC panels with intermediate CNT volume fraction do not necessarily have intermediate nonlinear to linear frequency ratios.

In structural engineering, the problem of plates supported by elastic foundations is investigated by many researchers [22,23]. Two main models are commonly used to represent the interaction between the plate and the foundation. In Winkler or one-parameter model [24], the interaction is solely represented by series of separated spring. Adding shear springs, this model was improved by Pasternak or two-parameter model [25] to account for more realistic interaction between separated springs. Several more studies considering functionally graded (FG) plates on elastic foundations include [26-28].

In this article, buckling analysis of FG-CNTRC plates resting on elastic foundations based on FSDT subjected to in-plane loads is analyzed using the EFG method. Material properties of FG-CNTRCs are assumed to be temperature-dependent and vary continuously along the plate thickness direction. Uniform and three types of functionally graded distributions of CNTs are considered. The principle of minimum potential energy is employed to obtain Galerkin weak-form formulation of the FG-CNTRC plate on two-parameter elastic foundations. The full transformation method is applied to impose essential boundary conditions. The effects of distribution and volume fractions of CNTs, plate width-to-thickness ratio, plate aspect ratio as well as parameters of elastic foundation and temperature change under various boundary conditions on the buckling behavior of FG-CNTRC plates are investigated.

2 CARBON NANOTUBE-REINFORCED COMPOSITES

Consider a CNTRC plate with length a , width b and thickness h on an elastic foundation (Fig. 1). The plate is made

of mixture of SWCNTs and an isotropic matrix. Employing the rule of mixture the effective elastic properties of the CNTRC plate can be expressed as follows [14]

$$E_{11} = \eta_1 V_{CNT} E_{11}^{CNT} + V_m E^m, \tag{1}$$

$$\frac{\eta_2}{E_{22}} = \frac{V_{CNT}}{E_{22}^{CNT}} + \frac{V_m}{E^m}, \tag{2}$$

$$\frac{\eta_3}{G_{12}} = \frac{V_{CNT}}{G_{12}^{CNT}} + \frac{V_m}{G^m}, \tag{3}$$

where E_{11}^{CNT}, E_{22}^{CNT} denote Young's moduli of the CNTs in the longitudinal and transverse directions, respectively and G_{12}^{CNT} is its shear modulus. E^m and G^m are the corresponding properties of the isotropic matrix. η_j $(j = 1,2,3)$ are the CNT efficiency parameters accounting for the scale-dependent material properties evaluated by comparing the effective material properties obtained from MD simulations and that of numerical results [14]. Moreover, the Poisson's ratio is assumed to be constant and expressed as:

$$\nu_{12} = V_{CNT}^* \nu_{12}^{CNT} + V_m \nu^m, \tag{4}$$

where ν_{12}^{CNT} and ν^m are Poisson's ratios of the CNT and the matrix, respectively. V_{CNT} and V_m are the CNT and matrix volume fractions related by

$$V_{CNT} + V_m = 1. \tag{5}$$

The SWCNTs are either uniformly distributed (UD) or functionally graded (FG) along the thickness direction according to Eqs. (6) for V-, O- and X- distribution types as shown in Figs. 1.

$$V_{CNT} = \begin{cases} V_{CNT}^* & (\text{UD CNTRC}), \\ \left(1 + \dfrac{2z}{h}\right) V_{CNT}^* & (\text{FG-V CNTRC}), \\ 2\left(1 - \dfrac{2|z|}{h}\right) V_{CNT}^* & (\text{FG-O CNTRC}), \\ 2\left(\dfrac{2|z|}{h}\right) V_{CNT}^* & (\text{FG-X CNTRC}), \end{cases} \tag{6}$$

where

$$V_{CNT}^* = \frac{w_{CNT}}{w_{CNT} + (\rho^{CNT} / \rho^m)(1 - w_{CNT})}. \tag{7}$$

V_{CNT}^* is the CNT volume fraction in which w_{CNT}, ρ^{CNT} and ρ^m are the mass fraction of CNTs, densities of CNTs and matrix, respectively. It is to be noted that for both UD and FG cases the values of mass fractions of CNTs are considered to be the same. Similarly, the thermal expansion coefficients in either material coordinates are as follows:

$$\alpha_{11} = V_{CNT} \alpha_{11}^{CNT} + V_m \alpha^m, \tag{8}$$

$$\alpha_{22} = (1+\nu_{12}^{CNT})V_{CNT}\alpha_{22}^{CNT} + (1+\nu^{m})V_{m}\alpha^{m} - \nu_{12}\alpha_{11}, \tag{9}$$

where α_{11}^{CNT}, α_{22}^{CNT} and α^{m} are thermal expansion coefficients of the CNT and the matrix, respectively. It should be noted that α_{11} and α_{22} are graded along thickness direction. According to these considerations, the elastic properties of the CNTs and the matrix are temperature-dependent.

3 THE EFG FORMULATION

According to MLS approximation, an unknown scalar function, $u(\mathrm{x})$, defined in the domain Ω can be approximated by $u^{h}(\mathrm{x})$ as follows:

$$u^{h}(\mathrm{x}) = \sum_{j=1}^{m} p_{j}(\mathrm{x})a_{j}(\mathrm{x}) = \mathrm{p}^{\mathrm{T}}(\mathrm{x})\mathrm{a}(\mathrm{x}), \tag{10}$$

In which $\mathrm{p}(\mathrm{x})$ is the basis function of spatial coordinates, $\mathrm{a}(\mathrm{x})$ is a vector of coefficients, and *m* is the number of basis functions. The quadratic bases commonly used are

$$\mathrm{p}^{\mathrm{T}} = [1, \mathrm{x}, \mathrm{x}^{2}] \quad \text{in 1D}, \mathrm{m} = 3, \qquad \mathrm{p}^{\mathrm{T}} = [1, \mathrm{x}, \mathrm{y}, \mathrm{x}^{2}, \mathrm{xy}, \mathrm{y}^{2}] \quad \text{in 2D}, \mathrm{m} = 6. \tag{11}$$

The unknown coefficients $a_{j}(\mathrm{x})$ can be determined by minimizing the following weighted discrete L_{2} norm

$$J = \sum_{i=1}^{n} \bar{W}(\mathrm{x} - \mathrm{x}_{i})[\mathrm{p}(\mathrm{x}_{i})^{\mathrm{T}}\mathrm{a}(\mathrm{x}) - \mathrm{u}_{i}]^{2} \tag{12}$$

where $\bar{W}(\mathrm{x} - \mathrm{x}_{i})$ or $\bar{W}_{i}(\mathrm{x})$ is the weight function associated with node *i*, *n* is the number of nodes in Ω, and u_{i} is the nodal parameter. Minimizing *J* in Eq. (10) with respect to $\mathrm{a}(\mathrm{x})$ leads to a set of linear relations

$$\mathrm{A}(\mathrm{x})\mathrm{a}(\mathrm{x}) = \mathrm{B}(\mathrm{x})\mathrm{u}, \tag{13}$$

where

$$\mathrm{A}(\mathrm{x}) = \sum_{i=1}^{n} \bar{W}_{i}(\mathrm{x})\mathrm{p}(\mathrm{x}_{i})\mathrm{p}^{\mathrm{T}}(\mathrm{x}_{i}) \tag{14}$$

$$\mathrm{B}(\mathrm{x}) = [\bar{W}_{1}(\mathrm{x})\mathrm{p}(\mathrm{x}_{1}), \cdots, \bar{W}_{n}(\mathrm{x})\mathrm{p}(\mathrm{x}_{n})]. \tag{15}$$

The coefficients $\mathrm{a}(\mathrm{x})$ are then obtained from Eq. (11)

$$\mathrm{a}(\mathrm{x}) = \mathrm{A}^{-1}(\mathrm{x})\mathrm{B}(\mathrm{x})\mathrm{u}. \tag{16}$$

Substituting Eq. (14) into Eq. (8), the approximation $u^{h}(\mathrm{x})$ can be expressed in a standard form as:

$$u^{h}(\mathrm{x}) = \sum_{i=1}^{n} \phi_{i}(\mathrm{x})u_{i}, \tag{17}$$

where the shape function for node *i*, denoted by $\phi_{i}(\mathrm{x})$ is given by

$$\phi_i(\mathrm{x}) = \sum_{j=1}^{m} p_j(\mathrm{x})\left(\mathrm{A}^{-1}(\mathrm{x})\mathrm{B}(\mathrm{x})\right)_{ji} = \mathrm{p}^{\mathrm{T}}\left(\mathrm{A}^{-1}\mathrm{B}\right)_i . \tag{18}$$

A quintic spline weight function is defined as:

$$\bar{W}_i(\mathrm{x}) = \begin{cases} 1-10\bar{r}_i^2+20\bar{r}_i^3-15\bar{r}_i^4+4\bar{r}_i^5; & 0 \le \bar{r}_i < 1 \\ 0 \quad ; & \bar{r}_i \ge 1 \end{cases}, \tag{19}$$

where

$$\bar{r}_i = \frac{\left|\mathrm{x}-\mathrm{x}_i\right|}{d_s}, \tag{20}$$

In which $\left|\mathrm{x}-\mathrm{x}_i\right|$ is the distance from node x_i to the sampling point *x*, and d_s is the size of support domain for the sampling point *x*.

4 GOVERNING EQUATIONS OF CNTRC PLATES RESTING ON ELASTIC FOUNDATIONS

4.1 Displacement field and strains

Employing the FSDT for a CNTRC plate, the displacement field of the plate can be expressed as:

$$u(x,y,z) = u_0(x,y) + z\,\varphi_x(x,y), \tag{21}$$

$$v(x,y,z) = v_0(x,y) + z\,\varphi_y(x,y), \tag{22}$$

$$w(x,y,z) = w_0(x,y), \tag{23}$$

where (u,v,w) are the displacements of an arbitrary point (x,y,z) in the domain of FG-CNTRC plate along x-, y- and z- directions, respectively. (u_0,v_0,w_0) represent the displacements of a point at the mid-plane of the plate and (φ_x,φ_y) denote rotations of the unit normal to the mid-plane of plate at the martial point (x,y) about positive y- and negative x- axes, respectively. The strains of the plate are given by

$$\varepsilon = \varepsilon^{(0)} + z\varepsilon^{(1)}, \tag{24}$$

$$\gamma = \gamma^{(0)}, \tag{25}$$

where

$$\varepsilon = [\varepsilon_{xx} \quad \varepsilon_{yy} \quad \gamma_{xy}]^{\mathrm{T}}, \gamma = [\gamma_{yz} \quad \gamma_{xz}]^{\mathrm{T}}, \tag{26}$$

and

$$\varepsilon^{(0)} = \begin{Bmatrix} \dfrac{\partial u_0}{\partial x} \\ \dfrac{\partial v_0}{\partial y} \\ \dfrac{\partial u_0}{\partial y}+\dfrac{\partial v_0}{\partial x} \end{Bmatrix}, \varepsilon^{(1)} = \begin{Bmatrix} \dfrac{\partial \varphi_x}{\partial x} \\ \dfrac{\partial \varphi_y}{\partial y} \\ \dfrac{\partial \varphi_x}{\partial y}+\dfrac{\partial \varphi_y}{\partial x} \end{Bmatrix}, \tag{27}$$

and

$$\gamma^{(0)}=\begin{Bmatrix}\varphi_y+\dfrac{\partial w_0}{\partial y}\\ \varphi_x+\dfrac{\partial w_0}{\partial x}\end{Bmatrix}. \tag{28}$$

Then, the constitutive relations are expressed as:

$$\begin{Bmatrix}\sigma_{xx}\\ \sigma_{yy}\\ \sigma_{yz}\\ \sigma_{xz}\\ \sigma_{xy}\end{Bmatrix}=\begin{bmatrix}Q_{11}(z) & Q_{12}(z) & 0 & 0 & 0\\ Q_{12}(z) & Q_{22}(z) & 0 & 0 & 0\\ 0 & 0 & Q_{44}(z) & 0 & 0\\ 0 & 0 & 0 & Q_{55}(z) & 0\\ 0 & 0 & 0 & 0 & Q_{66}(z)\end{bmatrix}\left(\begin{Bmatrix}\varepsilon_{xx}\\ \varepsilon_{yy}\\ \gamma_{yz}\\ \gamma_{xz}\\ \gamma_{xy}\end{Bmatrix}-\begin{Bmatrix}\alpha_{11}\\ \alpha_{22}\\ 0\\ 0\\ 0\end{Bmatrix}\Delta T\right), \tag{29}$$

where

$$Q_{11}=\frac{E_{11}}{1-\nu_{12}\nu_{21}},Q_{22}=\frac{E_{22}}{1-\nu_{12}\nu_{21}},Q_{12}=\frac{\nu_{21}E_{11}}{1-\nu_{12}\nu_{21}},Q_{44}=\kappa_{23}G_{23},Q_{55}=\kappa_{13}G_{13},Q_{66}=G_{12}. \tag{30}$$

ΔT is the temperature change with respect to the reference state. E_{11} and E_{22} are the effective Young's moduli of a CNTRC plate in the principle material coordinates; G_{12},G_{13} and G_{23} are the shear moduli, and ν_{12} and ν_{21} are the Poisson's ratios. Note that $\nu_{21}=(E_{22}/E_{11})\nu_{12}$.

κ_{ij} are the modified shear correction factors evaluated based on energy equivalence principle involving the actual non-uniform shear stress distribution through the thickness of the FG-CNTRC plate and defined as [29]

$$\kappa_{ij}=\frac{\left(\int_{-(h/2)-d_i}^{(h/2)-d_i}\left(\int_{-(h/2)-d_i}^{z}E_{ii}(z)z dz\right)dz\right)^2}{\int_{-(h/2)-d_i}^{(h/2)-d_i}G_{ij}dz\int_{-(h/2)-d_i}^{(h/2)-d_i}\dfrac{\left(\int_{-(h/2)-d_i}^{z}E_{ii}(z)z dz\right)^2}{G_{ij}(z)}dz},\ i=1\text{or}\,2,\ j=3,(\text{no summation}), \tag{31}$$

where d_i are the distances of neutral surface from the mid-surface of the plate in the principle material coordinates given by

$$d_i=\frac{\int_{-h/2}^{h/2}zE_{ii}(z)dz}{\int_{-h/2}^{h/2}E_{ii}(z)dz},\ i=1\text{or}\,2\,(\text{no summation}). \tag{32}$$

According to FSDT, the relation between the stress resultants and the strains can be written as:

$$\begin{Bmatrix}\mathrm{N}\\ \mathrm{M}\\ \mathrm{Q}^{\mathrm{s}}\end{Bmatrix}=\begin{bmatrix}\mathrm{A} & \bar{\mathrm{B}} & 0\\ \bar{\mathrm{B}} & \mathrm{D} & 0\\ 0 & 0 & \mathrm{A}^{\mathrm{s}}\end{bmatrix}\begin{Bmatrix}\varepsilon^{(0)}\\ \varepsilon^{(1)}\\ \gamma^{(0)}\end{Bmatrix}-\begin{Bmatrix}\mathrm{N}^{th}\\ \mathrm{M}^{th}\\ 0\end{Bmatrix}, \tag{33}$$

where the in-plane force resultants, moment resultants, transverse force, thermal force resultants and thermal moment resultants are defined as:

$$\left(\mathrm{N},\mathrm{M}\right)=\begin{pmatrix}N_{xx},M_{xx}\\N_{yy},M_{yy}\\N_{xy},M_{xy}\end{pmatrix}=\int_{-h/2}^{h/2}(1,\mathrm{z})\begin{pmatrix}\sigma_{xx}\\\sigma_{yy}\\\sigma_{xy}\end{pmatrix}dz\ , \tag{34}$$

$$\mathrm{Q}^{\mathrm{s}}=\begin{Bmatrix}Q_y^s\\Q_x^s\end{Bmatrix}=\int_{-h/2}^{h/2}\begin{Bmatrix}\sigma_{yz}\\\sigma_{xz}\end{Bmatrix}dz\,, \tag{35}$$

$$\left(\mathrm{N}^{th},\mathrm{M}^{th}\right)=\begin{pmatrix}N_{xx}^{th},M_{xx}^{th}\\N_{yy}^{th},M_{yy}^{th}\\N_{xy}^{th},M_{xy}^{th}\end{pmatrix}=\int_{-h/2}^{h/2}(1,\mathrm{z})\begin{pmatrix}Q_{11}(z)&Q_{12}(z)&0\\Q_{12}(z)&Q_{22}(z)&0\\0&0&Q_{66}(z)\end{pmatrix}\begin{pmatrix}\alpha_{11}\\\alpha_{22}\\0\end{pmatrix}\Delta T dz\ . \tag{36}$$

The components of extensional A, bending-extensional coupling $\bar{\mathrm{B}}$, bending D and transverse shear A^{s} stiffnesses are defined as:

$$\left(A_{ij},\bar{B}_{ij},D_{ij}\right)=\int_{-h/2}^{h/2}Q_{ij}\left(1,z,z^2\right)dz\quad\text{for } i,j=1,2\,\text{and}\,6, \tag{37}$$

$$A_{ij}^{s}=\int_{-h/2}^{h/2}Q_{ij}dz\quad\text{for } i,j=4\,\text{and}\,5. \tag{38}$$

4.2 Stiffness matrices

Total potential energy of the plate resting on an elastic foundation subjected to a transverse load is expressed as:

$$\Pi=\mathrm{U}_p+\mathrm{U}_f-\mathrm{W}, \tag{39}$$

where U_p and U_f denote the strain energies of the plate and the foundation, respectively. W is the work done by external forces. The strain energy of the plate can be written as:

$$\mathrm{U}_p=\frac{1}{2}\int_{\Omega}\varepsilon_p^{\mathrm{T}}\mathrm{S}_p\,\varepsilon_p\,d\Omega, \tag{40}$$

where

$$\varepsilon_p=\begin{Bmatrix}\varepsilon^{(0)}\\\varepsilon^{(1)}\\\gamma^{(0)}\end{Bmatrix},\mathrm{S}_p=\begin{bmatrix}\mathrm{A}&\bar{\mathrm{B}}&0\\\bar{\mathrm{B}}&\mathrm{D}&0\\0&0&\mathrm{A}^{\mathrm{s}}\end{bmatrix}. \tag{41}$$

The strain energy of the foundation can be expressed as:

$$\mathrm{U}_f=\frac{1}{2}\int_{\Omega}\varepsilon_f^{T}\mathrm{S}_f\,\varepsilon_f\,d\Omega, \tag{42}$$

where

$$\varepsilon_f = \begin{Bmatrix} w_0 \\ \dfrac{\partial w_0}{\partial x} \\ \dfrac{\partial w_0}{\partial y} \end{Bmatrix}, \mathrm{S}_f = \begin{bmatrix} k_F & 0 & 0 \\ 0 & k_G & 0 \\ 0 & 0 & k_G \end{bmatrix}, \tag{43}$$

where k_F and k_G are Winkler and the shear stiffnesses of an elastic foundation, respectively. It should be mentioned that the foundation is assumed to be compliant which implies that no parts of the plate lift off the foundation. Considering the in-plane loads, $\gamma_1 R_x$ and $\gamma_2 R_y$ as depicted in Fig. 1 applied on the plate, W can be expressed as:

$$\mathrm{W} = \int_\Omega \begin{bmatrix} \dfrac{\partial w}{\partial x} & \dfrac{\partial w}{\partial y} \end{bmatrix} \begin{bmatrix} \gamma_1 R_x & 0 \\ 0 & \gamma_2 R_y \end{bmatrix} \begin{bmatrix} \dfrac{\partial w}{\partial x} \\ \dfrac{\partial w}{\partial y} \end{bmatrix} d\Omega. \tag{44}$$

Substituting Eq. (40), Eq. (42) and Eq. (44) into Eq. (39) and following the standard procedure of EFG method the following system of eigenvalue equations is derived.

$$(\mathrm{K} - \lambda \mathrm{K}^g)\mathrm{u} = 0, \tag{45}$$

where λ is the critical buckling load of the plate resting on an elastic foundation, K^g is the geometric stiffness matrix and

$$\mathrm{K} = \mathrm{K}^p + \mathrm{K}^f, \tag{46}$$

In which K^p and K^f denote the global stiffness matrices of the plate and the foundation, respectively; given by

$$\mathrm{K}^p = \mathrm{K}^m + \mathrm{K}^b + \mathrm{K}^s + \mathrm{K}^c, \tag{47}$$

$$\mathrm{K}_{ij}^m = \int_\Omega \mathrm{B}_i^{m^T} \mathrm{A} \mathrm{B}_j^m \mathrm{d}\Omega, \tag{48}$$

$$\mathrm{K}_{ij}^b = \int_\Omega \mathrm{B}_i^{b^T} \mathrm{D} \mathrm{B}_j^b \mathrm{d}\Omega, \tag{49}$$

$$\mathrm{K}_{ij}^s = \int_\Omega \mathrm{B}_i^{s^T} \mathrm{A}^s \mathrm{B}_j^s \mathrm{d}\Omega, \tag{50}$$

$$\mathrm{K}_{ij}^c = \int_\Omega \mathrm{B}_i^{m^T} \bar{\mathrm{B}} \mathrm{B}_j^b \mathrm{d}\Omega + \int_\Omega \mathrm{B}_i^{b^T} \bar{\mathrm{B}} \mathrm{B}_j^m \mathrm{d}\Omega, \tag{51}$$

$$\mathrm{K}_{ij}^f = \begin{bmatrix} 0 & 0 & 0 & 0 & 0 \\ 0 & 0 & 0 & 0 & 0 \\ 0 & 0 & L_{ij} & 0 & 0 \\ 0 & 0 & 0 & 0 & 0 \\ 0 & 0 & 0 & 0 & 0 \end{bmatrix}, \tag{52}$$

$$L_{ij} = \int_\Omega \mathrm{B}_i^{f^T} \mathrm{S}_f \mathrm{B}_j^f \mathrm{d}\Omega, \tag{53}$$

$$K_{ij}^{g} = \int_{\Omega} H_i^{T} R H_j \, d\Omega, \tag{54}$$

In which

$$B^{m} = \begin{bmatrix} \phi_{i,x} & 0 & 0 & 0 & 0 \\ 0 & \phi_{i,y} & 0 & 0 & 0 \\ \phi_{i,y} & \phi_{i,x} & 0 & 0 & 0 \end{bmatrix}, \tag{55}$$

$$B^{b} = \begin{bmatrix} 0 & 0 & 0 & \phi_{i,x} & 0 \\ 0 & 0 & 0 & 0 & \phi_{i,y} \\ 0 & 0 & 0 & \phi_{i,y} & \phi_{i,x} \end{bmatrix}, \tag{56}$$

$$B^{s} = \begin{bmatrix} 0 & 0 & \phi_{i,y} & 0 & \phi_i \\ 0 & 0 & \phi_{i,x} & \phi_i & 0 \end{bmatrix}, \tag{57}$$

$$B^{f} = \begin{bmatrix} \phi_i & \phi_{i,x} & \phi_{i,y} \end{bmatrix}, \tag{58}$$

$$H = \begin{bmatrix} 0 & 0 & \phi_{i,x} & 0 & 0 \\ 0 & 0 & \phi_{i,y} & 0 & 0 \end{bmatrix}, \tag{59}$$

$$R = \begin{bmatrix} \gamma_1 R_x & 0 \\ 0 & \gamma_2 R_y \end{bmatrix}. \tag{60}$$

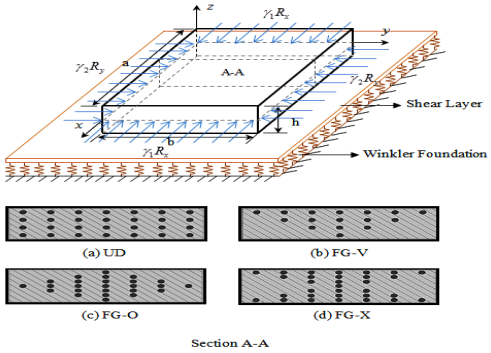

Fig.1
Schematic configuration of a carbon nanotube-reinforced composite plate resting on an elastic foundation with four types of CNT distributions: (a) UD CNTRC (b) FG-V CNTRC (c) FG-O CNTRC (d) FG-X CNTRC.

5 BOUNDARY CONDITIONS

The essential boundary conditions cannot be directly imposed in EFG method due to the fact that the MLS shape functions do not satisfy the Kronecker delta property. Several approaches are used to impose boundary conditions including the Lagrangian multiplier method [30] and the penalty method [31]. The adopted method used in this paper is the full transformation method proposed by Chen et al. [32] and used by many researchers, e.g. [18], [20] and [33] due to its good accuracy and simple implementation.

The boundary conditions considered in this study are as follows:

Simply supported (S)

$$\begin{aligned} v_0 &= w_0 = \varphi_y = 0, \text{ at } x = 0, a, \\ u_0 &= w_0 = \varphi_x = 0, \text{ at } y = 0, b. \end{aligned} \tag{61}$$

Clamped (C)

$$\begin{aligned} &v_0 = w_0 = \varphi_x = \varphi_y = 0, \text{ at } x = 0, a, \\ &u_0 = w_0 = \varphi_x = \varphi_y = 0, \text{ at } y = 0, b. \end{aligned} \tag{62}$$

The supports of the plate edges are denoted by *S*, *C* or *F* for simply supported, clamped or free boundary conditions, respectively.

6 NUMERICAL RESULTS AND DISCUSSION

In this section, to examine the convergency and accuracy of the present method; firstly, the buckling load parameters of isotropic and CNTRC plates are presented and compared with previous studies. Then to demonstrate the effects of elastic foundation parameters, CNT volume fraction and distribution, and width-to-thickness and aspect ratios of the plate, temperature changes as well as boundary conditions on the buckling behavior of the CNTRC plates resting on elastic foundations several parametric studies are presented and investigated in detail.

6.1 Convergence study and validation

The buckling problem of isotropic plates resting on elastic foundations is presented to investigate the convergency and accuracy of the present method. The results are listed in Table 1. for a plate without any elastic foundation, Winkler and Pasternak elastic foundations using various node schemes. The elastic foundation parameters (K_1, K_2) are defined as:

$$K_1 = \frac{k_f b^4}{D}, \qquad K_2 = \frac{k_G b^2}{D} \tag{63}$$

where $D = Eh^3/12(1-\nu^2)$ is the flexural rigidity of an isotropic plate. The results are compared with that of presented by Lam et al. [22] and Malekzadeh et al. [34]. As can be seen, the solution converges when the number of nodes is increased and the results are converged with 21×21 regular nodal distribution. Accordingly, this node scheme is used for discretization of the domain in the following studies. Moreover, following numerical experiments, the dimensionless sizes of rectangular support domains along x- and y-directions are chosen to be $\alpha_{sx} = \alpha_{sy} = d_s / d_c = 3.2$ where d_s is defined in Eq. (20) and d_c is the nodal spacing near the point of interest.

The problem of a CNTRC square plate with all edges simply supported (SSSS) subjected to the uniaxial $(\gamma_1 = -1, \gamma_2 = 0)$ and biaxial $(\gamma_1 = -1, \gamma_2 = -1)$ compressive loads is considered to examine the accuracy of the present numerical method. Buckling load parameters $(\bar{N}_{cr} = N_{cr} b^2 / E^m \text{ h}^3)$ are presented in Table 2. for the first four modes. The geometrical and material properties of the plate are considered as mentioned in [20]. It can be seen that the obtained results are in good agreement with the reported results in [20].

Table 1
Convergence study of critical buckling load parameters $(N^*_{cr} = N_{cr} b^2 / D\pi^2)$ for an isotropic square plate (h/ a = 0.01, $\nu = 0.3$) on elastic foundations subjected to a uniaxial compressive load $(\gamma_1 = -1, \gamma_2 = 0)$.

		(K_1, K_2)		
	Number of Nodes	(0,0)	(100,0)	(100,100)
Present	13×13	4.0115	5.0448	19.2488
	15×15	4.0118	5.0427	19.2575
	17×17	4.0134	5.0430	19.2729
	19×19	4.0002	5.0288	19.1797
	21×21	4.0002	5.0288	19.1797
Ref [22]		4.000	5.027	19.17
Ref [34]		4.000	5.027	19.172

Table 2
Comparison study of buckling load parameters ($\bar{N}_{cr} = N_{cr} b^2 / E^m \mathrm{h}^3$) for a simply supported isotropic square plate subjected to uniaxial and biaxial compressive loads ($V^*_{CNT} = 0.11$, b/ h = 20).

Mode		Uniaxial Compression $(\gamma_1 = -1, \gamma_2 = 0)$			Biaxial Compression $(\gamma_1 = -1, \gamma_2 = -1)$		
		UD	FG-O	FG-X	UD	FG-O	FG-X
1	Present	31.1572	18.7988	40.8191	9.5615	7.0039	11.6256
	Ref [20]	30.9076	18.7534	40.8005	9.3805	6.9161	11.4231
2	Present	47.9739	35.1408	58.3313	10.6664	9.1219	12.0071
	Ref [20]	46.9779	34.4733	57.3978	10.3981	8.9197	11.6524
3	Present	70.5572	49.5965	81.6055	14.5637	9.3992	15.8074
	Ref [20]	69.3955	48.4971	82.0077	14.0470	9.3380	15.0540
4	Present	76.3942	55.8230	87.3672	15.5780	13.1982	20.4082
	Ref [20]	74.5610	54.0994	86.8162	15.3108	12.7496	19.6846

6.2 Parametric studies

In the following, buckling analysis of CNTRC plates resting on two-parameter elastic foundations subjected to in-plane loads is presented. Buckling load parameters ($\bar{N}_{cr} = N_{cr} b^2 / E^m h^3$) of CNTRC plates under uniaxial compression $(\gamma_1 = -1, \gamma_2 = 0)$, biaxial compression $(\gamma_1 = -1, \gamma_2 = -1)$ and biaxial compression and tension $(\gamma_1 = -1, \gamma_2 = 1)$ are listed in Table 5-7. for various boundary conditions. Poly methyl methacrylate, referred to as PMMA and (10,10) SWCNTs are selected as the matrix and the reinforcement materials, respectively. Four types of uniform, FG-V, FG-O and FG-X CNT arrangements are considered. The material properties of CNTs are listed in Table 3. in various temperatures. The elastic properties of PMMA matrix are considered as: $\nu^m = 0.34$, $\alpha^m = 45(1 + 0.0005\Delta \mathrm{T}) \times 10^{-6} / \mathrm{K}$ and $E^m = (3.52 - 0.0034T)\mathrm{GPa}$, in which $T = T_0 + \Delta T$ and $T_0 = 300\mathrm{K}$ is the room temperature. Values of $\eta_i \, (i = 1, 2 \text{and } 3)$ for different CNT volume fractions are presented in Table 4. Note that $\eta_3 = 0.7\eta_2$, $G_{13} = G_{12}$ and $G_{23} = 1.2G_{12}$ following the assumptions mentioned in [35]. The CNT volume fraction is considered to be $V^*_{CNT} = 0.12$. The plate width-to-thickness ratio and thickness are taken to be $b / h = 10$ and $h = 2.0\,\mathrm{mm}$. The effects of Winkler and Pasternak foundations considering the influence of each elastic foundation parameter on buckling behavior of CNTRC plates subjected to in-plane loads are investigated. Note that for CNTRC plates, *D* defined in Eq. (63) is replaced by D^m which is the flexural rigidity of an isotropic plate made of polymer matrix.

It can be seen that as more constrains are applied on the edges of the plate the buckling load parameters are increased. Thus the minimum values of buckling load parameters occurred in SFSF boundary conditions and the maximum ones correspond to CCCC boundary conditions. In addition, elastic foundation parameters have significant influence on the buckling load parameters of the CNTRC plates. In other words, adding elastic foundations increases the stability of the plates subjected to various types of in-plane loads. Due to considering the shear layer in Pasternak elastic foundations, the buckling load parameters correspond to this type of elastic foundation is greater than that of Winkler elastic foundation. Moreover, the most and the least stable CNTRC plates on elastic foundations correspond to FG-X and FG-O distribution of CNTs, respectively. This behavior can be justified by the fact that in an FG-X CNT arrangement, the CNTs are denser close to the top and bottom of the CNTRC plate which leads to higher plate stiffness. Comparing the results in Tables 5-7. shows that the buckling load parameters of biaxial compression and tension load $(\gamma_1 = -1, \gamma_2 = 1)$ are higher than the other two load cases. It implies that applying the tension load along two opposite edges of the plate while the other two edges are under compression increases the buckling load parameters of the plate.

Table 3
Elastic properties of the (10,10) SWCNT in various temperatures ($\nu_{12}^{CNT} = 0.175$) [35].

Temperature (K)	E_{11}^{CNT} (TPa)	E_{22}^{CNT} (TPa)	G_{12}^{CNT} (TPa)	α_{11}^{CNT} ($\times 10^{-6}$/K)	α_{22}^{CNT} ($\times 10^{-6}$/K)
300	5.6466	7.0800	1.9445	3.4584	5.1682
500	5.5308	6.9348	1.9643	4.5361	5.0189
700	5.4744	6.8641	1.9644	4.6677	4.8943
1000	5.2814	6.6220	1.9451	4.2800	4.7532

Table 4
CNT efficiency parameters for different values of volume fractions[35].

V^*_{CNT}	η_1	η_2	η_3
0.12	0.137	1.022	0.715
0.17	0.142	1.626	1.138
0.28	0.141	1.585	1.109

Table 5
Buckling load parameters $(\bar{N}_{cr} = N_{cr}b^2 / E^m h^3)$ of CNTRC square plate resting on elastic foundations with various boundary conditions under uniaxial compression load $(\gamma_1 = -1, \gamma_2 = 0)$.

		(K_1, K_2)											
	Mode	(0,0)				(200,0)				(200,20)			
		Boundary Conditions				Boundary Conditions				Boundary Conditions			
		SSSS	SCSC	CCCC	SFSF	SSSS	SCSC	CCCC	SFSF	SSSS	SCSC	CCCC	SFSF
UD	1	15.6687	19.0022	23.2837	13.9767	17.5807	20.9135	23.7434	15.8856	21.3491	24.9620	26.1200	17.7766
	2	21.6627	22.4830	23.5303	14.5864	22.1407	22.9610	23.9677	16.4954	24.4942	25.3773	26.2132	20.5328
	3	23.5875	23.9406	24.6433	21.0218	23.8000	24.1531	24.7728	21.4990	25.8915	26.2686	26.8047	23.3855
	4	24.3504	24.5385	24.7786	21.2969	24.4693	24.6574	24.8874	21.8879	26.4686	26.6677	26.8693	24.2975
FG-V	1	12.9297	16.2986	20.7859	11.1216	14.8416	18.2101	21.2391	13.0306	18.6100	22.2562	23.6073	14.9233
	2	18.9200	19.7484	20.9220	11.7937	19.3980	20.2265	21.4147	13.7027	21.7515	22.6413	23.6977	17.7481
	3	21.0958	21.4517	22.3411	18.2229	21.3083	21.6642	22.4739	18.7002	23.3998	23.7791	24.5087	20.5877
	4	21.9953	22.1846	22.4731	18.6428	22.1142	22.3034	22.5943	19.1202	24.1135	24.3134	24.5840	21.5337
FG-O	1	11.0258	14.2375	19.2196	9.2541	12.9378	16.1492	19.7067	11.1630	16.7063	20.2030	22.0740	13.0575
	2	17.1532	17.9480	19.2579	9.9352	17.6312	18.4261	19.8118	11.8442	19.9847	20.8418	22.1651	15.8906
	3	19.6411	19.9848	21.1236	16.4446	19.8536	20.1973	21.2584	16.9218	21.9452	22.3125	23.2945	18.8106
	4	20.7170	20.9010	21.2378	16.6531	20.8359	21.0199	21.3833	17.3474	22.8352	23.0301	23.3884	19.7644
FG-X	1	18.1843	21.6867	24.4050	16.5002	20.0962	23.5959	24.8631	18.4092	23.8641	26.8287	27.1624	20.2982
	2	23.0787	23.9360	24.6666	17.0750	23.5566	24.4138	24.9871	18.9840	25.9101	27.1526	27.1887	23.0174
	3	24.4587	24.8255	25.2289	22.4518	24.6712	25.0379	25.3581	22.9291	26.7627	27.3027	27.3847	24.8147
	4	24.9801	25.1739	25.3241	22.8341	25.0990	25.2928	25.4145	23.3115	27.0983	27.3810	27.3894	25.7175

Table 6
Buckling load parameters $(\bar{N}_{cr} = N_{cr}b^2 / E^m h^3)$ of CNTRC square plate resting on elastic foundations with various boundary conditions under uniaxial compression load $(\gamma_1 = -1, \gamma_2 = -1)$.

		(K_1, K_2)											
	Mode	(0,0)				(200,0)				(200,20)			
		Boundary Conditions				Boundary Conditions				Boundary Conditions			
		SSSS	SCSC	CCCC	SFSF	SSSS	SCSC	CCCC	SFSF	SSSS	SCSC	CCCC	SFSF
UD	1	6.0349	7.8678	8.9298	3.2024	6.4177	8.2137	9.2303	3.4389	8.3022	10.0982	11.1149	5.3234
	2	7.8338	7.8967	9.5777	3.6961	8.1068	8.4455	9.9042	3.8705	9.9914	10.3300	11.7888	5.7550
	3	7.9155	11.2179	12.8419	7.3003	8.7900	11.6077	13.3086	7.3796	10.6745	13.4922	15.1931	9.2642
	4	10.7641	12.9278	13.1563	7.4125	10.876	13.0914	13.3136	7.4889	12.7607	14.9759	15.1981	9.3735
FG-V	1	5.5687	6.9718	8.5746	2.8812	5.9515	7.6458	8.8813	3.1318	7.8360	9.5303	10.7658	5.0163
	2	6.4646	7.5347	9.0977	3.4344	7.4206	7.8567	9.4990	3.6492	9.3051	9.7412	11.3835	5.5337
	3	7.7570	10.8374	12.2293	6.6227	7.9484	11.1639	12.5614	6.9729	9.8329	13.0484	14.4459	8.8574
	4	10.7351	12.0480	12.3863	6.8873	10.847	12.2305	12.7013	7.0861	12.7317	14.1150	14.5859	8.9707
FG-O	1	5.0582	6.1629	8.0787	2.5693	5.4409	6.8777	8.3874	2.8263	7.3254	8.7622	10.2720	4.7108
	2	5.5127	7.0041	8.5289	3.0922	6.4688	7.3280	8.9672	3.3381	8.3533	9.2125	10.8517	5.2226
	3	7.3147	10.2736	11.5755	5.7636	7.5062	10.5738	11.8752	6.5186	9.3907	12.4583	13.7597	8.4031
	4	10.3192	11.2386	11.6932	6.4301	10.431	11.4290	12.0389	6.5910	12.3158	13.3135	13.9234	8.4755
FG-X	1	6.6510	8.5124	9.3649	3.5670	7.0337	8.8259	9.6638	3.7951	8.9183	10.7104	11.5484	5.6797
	2	8.4059	8.7388	10.0101	4.0383	8.5974	9.2418	10.3254	4.1997	10.4819	11.1263	12.2099	6.0842
	3	9.0915	11.9734	13.3743	7.6816	10.047	12.4017	13.7951	7.7593	11.9320	14.2862	15.6797	9.6438
	4	11.2055	13.5375	13.6601	7.7935	11.317	13.6929	13.8146	7.8680	13.2021	15.5774	15.6991	9.7525

Table 7
Buckling load parameters $(\bar{N}_{cr} = N_{cr} b^2 / E^m h^3)$ of CNTRC square plate resting on elastic foundations with various boundary conditions under uniaxial compression load $(\gamma_1 = -1, \gamma_2 = 1)$.

Mode		(K_1, K_2)											
		(0,0)				(200,0)				(200,20)			
		Boundary Conditions				Boundary Conditions				Boundary Conditions			
		SSSS	SCSC	CCCC	SFSF	SSSS	SCSC	CCCC	SFSF	SSSS	SCSC	CCCC	SFSF
UD	1	25.3244	25.3275	25.3277	13.9873	25.3315	25.3345	25.3347	15.8967	27.2271	27.2300	27.2302	17.7815
	2	25.3324	25.3352	25.3355	21.0259	25.3390	25.3416	25.3419	21.5032	27.2337	27.2362	27.2363	23.3878
	3	25.3374	25.3416	25.3417	23.1867	25.3458	25.3499	25.3500	23.3989	27.2436	27.2476	27.2476	25.2835
	4	25.3445	25.3491	25.3493	24.0453	25.3528	25.3552	25.3555	24.1640	27.2470	27.2493	27.2497	26.0486
FG-V	1	23.1774	23.1815	23.1817	11.1350	23.1853	23.1891	23.1892	13.0445	25.0820	25.0853	25.0854	14.9294
	2	23.1849	23.1903	23.1908	18.2292	23.1941	23.1987	23.1992	18.7065	25.0921	25.0956	25.0960	20.5912
	3	23.1888	23.1945	23.1945	20.6670	23.1983	23.2025	23.2025	20.8792	25.0957	25.0997	25.0997	22.7638
	4	23.1888	23.1954	23.1959	21.6738	23.1992	23.2054	23.2057	21.7925	25.1004	25.1063	25.1064	23.6771
FG-O	1	22.0546	22.1886	22.1886	9.2697	22.1826	22.1991	22.1992	11.1794	24.0928	24.0984	24.0985	13.0645
	2	22.0588	22.1912	22.1912	16.4532	22.1897	22.2033	22.2033	16.9306	24.0988	24.1062	24.1065	18.8153
	3	22.1322	22.1964	22.1972	19.2096	22.1925	22.2079	22.2087	19.4218	24.1026	24.1103	24.1106	21.3064
	4	22.1584	22.1970	22.1982	20.3968	22.1974	22.2085	22.2097	20.5155	24.1031	24.1107	24.1114	22.4001
FG-X	1	25.6024	25.6048	25.6049	16.5077	25.6089	25.6112	25.6113	18.4170	27.5035	27.5057	27.5057	20.3016
	2	25.6045	25.6065	25.6066	22.4541	25.6104	25.6123	25.6124	22.9314	27.5040	27.5058	27.5059	24.8160
	3	25.6139	25.6162	25.6167	24.0592	25.6203	25.6226	25.6231	24.2714	27.5149	27.5168	27.5169	26.1559
	4	25.6152	25.6172	25.6173	24.6719	25.6211	25.6230	25.6231	24.7907	27.5152	27.5175	27.5181	26.6752

The variation of buckling load parameters for simply supported CNTRC plates resting on different types of elastic foundations under uniaxial compression $(\gamma_1 = -1, \gamma_2 = 0)$, biaxial compression $(\gamma_1 = -1, \gamma_2 = -1)$ and biaxial compression and tension $(\gamma_1 = -1, \gamma_2 = 1)$ versus CNT volume fraction are illustrated in Figs. 2. Three cases of foundations, i.e. no elastic foundation, Winkler and Pasternak elastic foundations are considered. The effect of UD and FG-X CNT distributions are investigated. The width-to-thickness and aspect ratios of the plates are taken to be $b/h = 10$ and $a/b = 10$, respectively. It can be seen that the buckling load parameters increase with increase in CNT volume fraction and its influence decreases for higher incremental increase in V^*_{CNT}. This phenomenon is more pronounced for biaxial compression and tension load case.

The variation of buckling load parameters of simply supported CNTRC plates resting on elastic foundations under uniaxial or biaxial in-plane loads versus plate width-to-thickness ratio are depicted in Figs. 3. It should be mentioned that in this case study the width of the plate, *b*, is set to be 20 in Eqs. (63), so that unique elastic foundation stiffinesses are applied for all *b/h* cases.

As expected, by increasing the plate width-to-thickness ratio the buckling load parameters are decreased for all in-plane load conditions.

The dependency of buckling load parameters to aspect ratio (a/b) of the simply supported CNTRC plates on elastic foundations is delineated in Figs. 4 for two types of CNT distributions. Three in-plane load cases are considered. The width-to-thickness ratio and CNT volume fraction of the plates are considered to be $b/h = 10$ and $V^*_{CNT} = 0.12$, respectively.

Fig. 4(a) which corresponds to uniaxial compressive load shows that the buckling load parameters of the plates oscillate and tend to reach constant values as plate aspect ratio is increased. Moreover, the effect of increasing plate aspect ratio reduces when the CNTRC plates rest on a Winkler or Pasternak elastic foundation. This behavior is identical for both the uniform and FG-X CNT configurations.

The buckling load parameters of biaxially compressed simply supported CNTRC plate decrease while plate aspect ratio is raised as shown in Fig. 4(b). Furthermore, the influence of plate aspect ratio on buckling load parameters of the plate is alleviated as the plate aspect ratio increase irrespective of their elastic foundation type.
The behavior of buckling load parameters is different when the compressive load on two opposite edges replaced by tension load (see Fig. 4(c)). It can be observed that the buckling load parameters of CNTRC plates increase gradually with increase in plate aspect ratio.

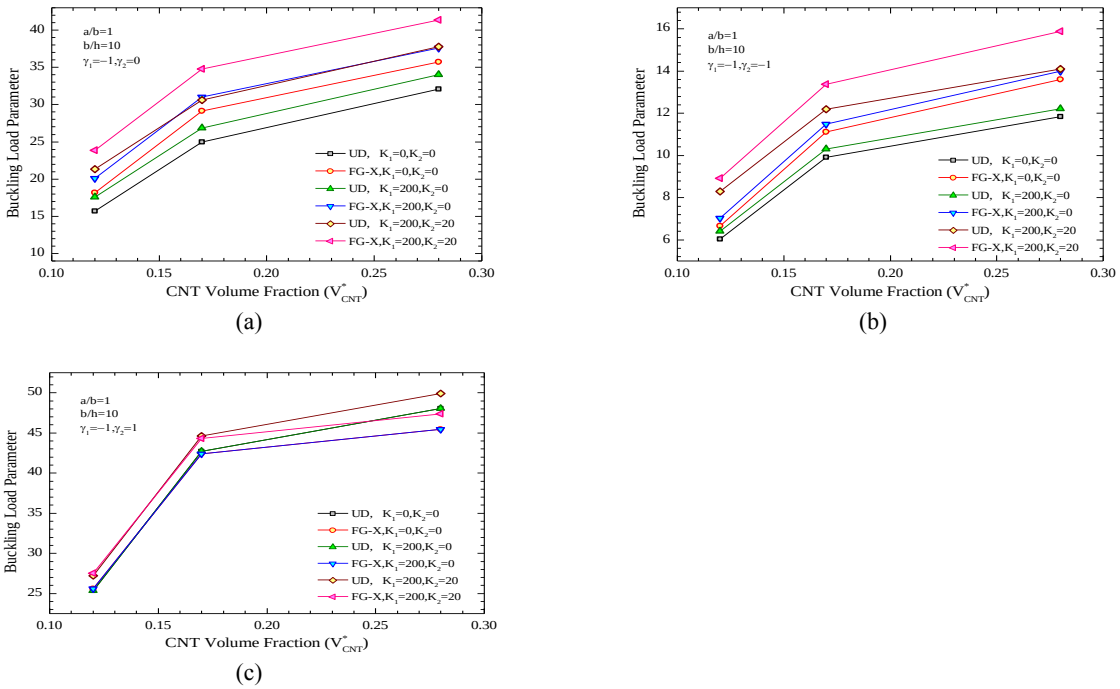

Fig.2
Effect of CNT volume fraction on the buckling load parameters of CNTRC square plates with all edges simply supported resting on different elastic foundations subjected to: a) uniaxial compression ($\gamma_1=-1,\gamma_2=0$), b) biaxial compression ($\gamma_1=-1,\gamma_2=-1$) and c) biaxial compression and tension ($\gamma_1=-1,\gamma_2=1$).

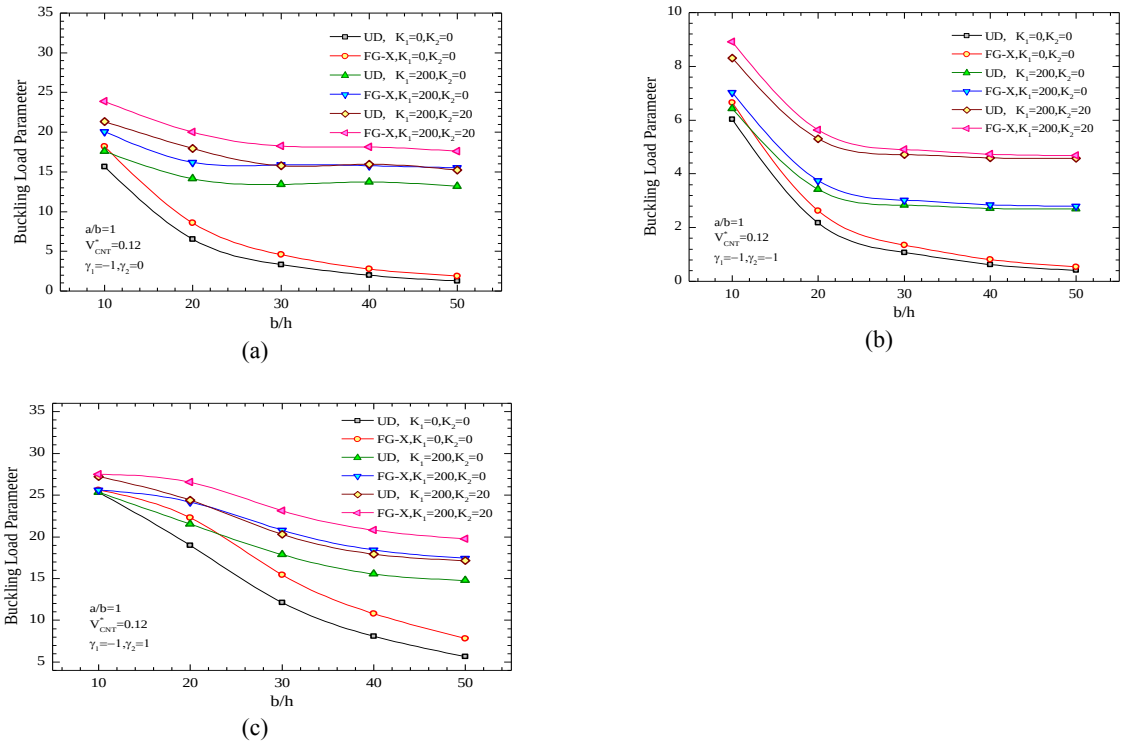

Fig.3
Variation of the buckling load parameters versus width-to-thickness ratios for simply supported CNTRC square plates resting on different elastic foundations subjected to: a) uniaxial compression ($\gamma_1=-1,\gamma_2=0$), b) biaxial compression ($\gamma_1=-1,\gamma_2=-1$) and c) biaxial compression and tension ($\gamma_1=-1,\gamma_2=1$).

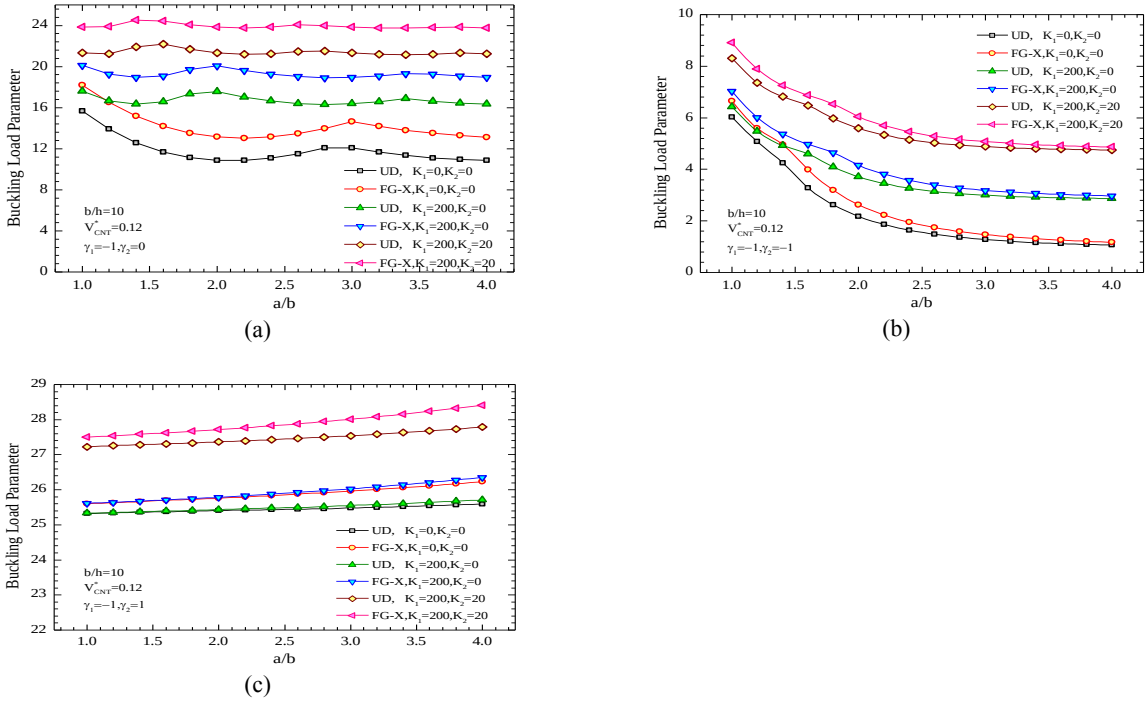

Fig 4

Variation of the buckling load parameters versus aspect ratios of simply supported CNTRC square plates resting on different elastic foundations subjected to: a) uniaxial compression ($\gamma_1=-1,\gamma_2=0$) , b) biaxial compression ($\gamma_1=-1,\gamma_2=-1$) and c) biaxial compression and tension ($\gamma_1=-1,\gamma_2=1$) .

The effects of temperature change on the buckling load parameters of the CNTRC square plate resting on elastic foundations for three types of in-plane loads are investigated in Tables 8-10. The width-to-thickness ratio and CNT volume fraction of the plate are set to be $b/h=20$ and $V^*_{CNT}=0.12$, respectively. It should be mentioned that in this case study the elastic modulus of the matrix, E^m used in Eqs. (63) is evaluated in $T=300\,\mathrm{K}$, so that unique elastic foundation stiffinesses are applied for all temperatures.

It is concluded that the temperature change has a significant influence on the buckling load parameters of the plate on an elastic foundation; i.e. as the temperature is raised the buckling load parameters are decreased. This is expectable because of the dependency of material properties of CNTs and the matrix on the temperature in which temperature rise attenuates the elastic moduli of both CNTs and the matrix. The dependency of the buckling load parameters of the plate on elastic foundation parameters is reconfirmed in Table 8-10.

Table 8

Buckling load parameters ($\bar{N}_{cr}=N_{cr}b^2/E^mh^3$) of CNTRC square plate resting on elastic foundations in various temperatures under uniaxial compression load ($\gamma_1=-1,\gamma_2=0$).

	(K_1,K_2)											
	(0,0)				(200,0)				(200,20)			
	Temperature (K)				Temperature (K)				Temperature (K)			
	300	500	700	1000	300	500	700	1000	300	500	700	1000
UD	26.1057	23.0876	19.0510	4.2124	28.0179	24.9998	20.9632	4.8606	31.7869	28.7687	24.7321	6.7492
	43.5887	35.6359	26.7181	4.6785	45.5088	37.5560	28.6380	4.8607	54.9617	47.0082	36.4850	6.7497
	56.9767	46.5687	33.6533	4.7784	57.4547	47.0467	34.1314	4.8612	59.8083	49.4003	38.0871	6.7507
	62.6708	50.5238	35.9689	4.8140	63.1508	51.0038	36.4489	4.8612	66.9196	54.7726	40.2174	6.7513
FG-V	19.7152	17.4657	14.6037	3.6418	21.6273	19.3779	16.5158	4.4063	25.3963	23.1468	20.2847	6.2952
	37.6975	30.3810	22.4989	4.1835	39.6175	32.3010	24.4188	4.4064	48.5081	40.7186	30.8812	6.2956
	45.6765	37.8870	28.0496	4.3050	46.1545	38.3650	28.5276	4.4069	49.0703	41.7530	33.8677	6.2965
	51.7224	42.0819	30.4921	4.3489	52.2024	42.5619	30.9721	4.4072	55.9712	46.3307	34.7407	6.2969
FG-O	15.8222	14.0845	11.9394	3.3200	17.7343	15.9966	13.8515	4.2198	21.5033	19.7656	17.6204	6.1092

	32.7486	26.2618	19.4047	3.9479	34.6687	28.1818	21.3247	4.2201	41.3140	35.2598	27.4418	6.1094
	38.4824	32.4282	24.6102	4.0155	38.9604	32.9062	25.0882	4.2208	44.1216	37.6341	30.7745	6.1104
	44.3617	36.5138	26.9873	4.0951	44.8417	36.9938	27.4673	4.2209	48.6106	40.7626	31.2359	6.1105
FG-X	34.2035	29.7376	23.7141	4.4681	36.1156	31.6498	25.6262	4.9141	39.8846	35.4187	29.3951	6.8026
	52.5930	42.9095	31.7468	4.7938	54.5130	44.8295	33.6665	4.9145	63.9654	54.2807	40.1374	6.8035
	66.9073	53.3885	37.3057	4.8606	67.3853	53.8665	37.7838	4.9151	69.7389	56.2201	43.1096	6.8047
	72.6406	57.3839	39.6654	4.8842	73.1206	57.8639	40.1454	4.9153	76.8894	61.6326	43.9136	6.8055

Table 9

Buckling load parameters $(\bar{N}_{cr} = N_{cr}b^2 / E^m h^3)$ of CNTRC square plate resting on elastic foundations in various temperatures under uniaxial compression load $(\gamma_1 = -1, \gamma_2 = -1)$.

	(K_1, K_2)											
	(0,0)				(200,0)				(200,20)			
	Temperature (K)				Temperature (K)				Temperature (K)			
	300	500	700	1000	300	500	700	1000	300	500	700	1000
UD	8.6877	7.1025	5.3250	0.7738	9.0704	7.4853	5.6656	0.9652	10.9549	9.3698	7.5501	2.8497
	10.6264	8.0934	5.4742	0.8651	10.8178	8.2848	5.7078	0.9771	12.7023	10.1693	7.5923	2.8616
	13.0525	11.1902	7.2205	0.9839	14.0085	11.3022	7.3325	1.1674	15.8930	13.1868	9.2170	3.0519
	15.1181	11.5433	9.5247	1.0936	15.2301	12.4993	9.8799	1.3661	17.1146	14.3839	11.7644	3.2506
FG-	7.5136	6.0553	4.4842	0.7211	7.8964	6.4380	4.8670	0.9126	9.7809	8.3226	6.7515	2.7971
	9.8573	7.6564	5.1061	0.8377	10.3519	7.8478	5.2976	0.9498	12.2364	9.7323	7.1821	2.8343
	10.1605	8.7326	7.0595	0.8725	10.8135	9.6887	7.1716	1.1530	12.6980	11.5732	9.0561	3.0375
	14.9784	11.0272	7.3015	1.0792	15.0905	11.1393	8.2576	1.2551	16.9750	13.0238	10.1421	3.1396
FG-	6.5273	5.2343	3.8676	0.6694	6.9101	5.6171	4.2503	0.8608	8.7946	7.5016	6.1348	2.7453
	7.9110	6.9899	4.6421	0.7861	8.8670	7.1815	4.8336	0.8981	10.7515	9.0660	6.7181	2.7826
	9.3103	7.0422	5.9695	0.8003	9.5018	7.9982	6.6947	1.0952	11.3863	9.8827	8.5792	2.9798
	14.0225	10.3054	6.5826	1.0215	14.1345	10.4175	6.9255	1.1829	16.0190	12.3020	8.8100	3.0675
FG-	10.4822	8.5521	6.1322	0.8215	10.8650	8.9348	6.3236	1.0129	12.7495	10.8194	8.2082	2.8974
	11.8833	9.0745	6.3272	0.9169	12.0747	9.2660	6.7099	1.0290	13.9592	11.1505	8.5944	2.9135
	16.3393	12.1147	7.8228	1.0438	16.4514	12.2267	7.9348	1.2278	18.3359	14.1112	9.8194	3.1124
	17.1009	14.8678	10.4448	1.1541	18.0570	15.8237	10.5186	1.4261	19.9415	17.7083	12.4031	3.3106

Table 10

Buckling load parameters $(\bar{N}_{cr} = N_{cr}b^2 / E^m h^3)$ of CNTRC square plate resting on elastic foundations in various temperatures under uniaxial compression load $(\gamma_1 = -1, \gamma_2 = 1)$.

	(K_1, K_2)											
	(0,0)				(200,0)				(200,20)			
	Temperature (K)				Temperature (K)				Temperature (K)			
	300	500	700	1000	300	500	700	1000	300	500	700	1000
UD	75.8529	61.9943	44.4724	4.8658	76.4890	62.6299	44.7100	4.8709	79.6216	65.7613	47.0552	6.7633
	84.3171	65.6575	44.7770	4.8666	84.5558	65.8961	45.0596	4.8723	86.9052	68.2453	47.1883	6.7657
	89.9926	68.3662	44.9349	4.8679	90.1192	68.4928	45.3731	4.8742	92.2480	70.6216	47.4390	6.7689
	93.5428	70.0818	45.3211	4.8687	93.6225	70.1614	45.4010	4.8757	95.6590	72.1980	47.5707	6.7716
FG-	60.8102	50.4389	37.3393	4.4109	61.4465	51.0750	37.9741	4.4160	64.5794	54.2075	41.1016	6.3085
	71.1395	56.0622	38.6115	4.4113	71.3781	56.3009	38.8499	4.4171	73.7276	58.6503	41.1989	6.3105
	78.1396	59.8438	39.7478	4.4124	78.2662	59.9704	39.8744	4.4188	80.3950	62.0992	42.0032	6.3134
	82.6092	62.2107	40.4922	4.4129	82.6889	62.2904	40.5719	4.4199	84.7254	64.3269	42.6085	6.3158
FG-	51.2332	43.1724	32.7628	4.2246	51.8695	43.8086	33.3986	4.2298	55.0025	46.9415	36.5301	6.1223
	62.7055	50.1307	35.2010	4.2247	62.9442	50.3693	35.4396	4.2306	65.2938	52.7188	37.7889	6.1241
	70.7981	54.8238	36.9200	4.2257	70.9247	54.9504	37.0465	4.2320	73.0535	57.0792	39.1753	6.1266
	76.1343	57.8086	37.9997	4.2260	76.2141	57.8883	38.0794	4.2329	78.2506	59.9248	40.1159	6.1287
FG-	89.0677	71.0532	46.5600	4.9194	89.7030	71.3420	46.5733	4.9244	92.8337	73.6897	48.4773	6.8168
	92.8961	71.1039	46.5618	4.9204	93.1346	71.6800	46.5747	4.9261	95.4838	74.3462	48.4803	6.8195
	96.0189	72.0930	46.5701	4.9219	96.1454	72.2199	46.5843	4.9283	98.2742	74.7647	48.4896	6.8230
	98.0327	72.8479	46.5714	4.9231	98.1124	72.9277	46.5860	4.9301	100.1489	74.9646	48.4909	6.8260

7 CONCLUSIONS

In the present study, buckling analysis of CNTRC plates resting on two-parameter elastic foundations has been investigated based on FSDT using the EFG method. The effective material properties of the plate were estimated based on a micromechanical model and the extended rule of mixture. The effects of various types of CNT distributions and volume fractions, plate width-to thickness and aspect ratio, elastic foundation parameters, temperature changes and boundary conditions have been studied. Based on present study the following results have been obtained.The results of EFG method conform the findings of previous works.

- Elastic foundation parameters have considerably decreased the values of the buckling load parameters of the plate.
- Increasing the width-to-thickness ratio of the plate decreases the buckling load parameter regardless of elastic foundation parameters.
- The variations of CNT volume fractions and distributions have noticeable effect on buckling behavior of CNTRC plates on elastic foundations.
- The more CNT is used in the plate; the higher buckling load parameters are achieved for all in-plane load conditions.
- The maximum and minimum values of buckling load parameters correspond to FG-X and FG-O CNT arrangements, respectively.
- The effect of plate aspect ratio is diminished for sufficiently large aspect ratios $(a/b > 3)$.
- The buckling load parameters decrease as the temperature rises.

REFERENCES

[1] Alibeigloo A., Liew K. M., 2013, Thermoelastic analysis of functionally graded carbon nanotube-reinforced composite plate using theory of elasticity, *Composite Structures* **106**: 873-881.

[2] Belytschko T., Lu Y. Y., Gu L., 1994, Element-free Galerkin methods, *International Journal of Numerical Methods in Engineering* **37**: 229-256.

[3] Bonnet P., Sireude D., Garnier B., Chauvet O., 2007, Thermal properties and percolation in carbon nanotube–polymer composites, *Journal of Applied Physics* **91**: 2019-2030.

[4] Chen J., Chunhui P., Wu C., Liu W., 1996, Reproducing kernel particle method for large deformation of nonlinear structures, *Computer Methods in Applied Mechanics and Engineering* **139**:195-227.

[5] Esawi A. M., Farag M. M., 2007, Carbon nanotube reinforced composites: potential and current challenges, *Materials & Design* **28**: 2394-2401.

[6] Fidelus J. D., Wiesel E., Gojny F. H., Schulte K., Wagner H. D., 2005, Thermo-mechanical properties of randomly oriented carbon/epoxy nanocomposites, *Composites Part A* **36**:1555-1561.

[7] Han J. B., Liew K. M., 1997, Numerical differential quadrature method for Reissner/Mindlin plates on two-parameter foundations, *International Journal of Mechanical Sciences* **39**(9): 977-989.

[8] Han Y., Elliott J., 2007, Molecular dynamics simulations of the elastic properties of polymer/carbon nanotube composites, *Computational Materials Science* **39**: 319-323.

[9] Hu N., Fukunaga H., Lu C., Kameyama M., Yan B., 2005, Prediction of elastic properties of carbon nanotube reinforced composites, *Proceeding Royal Society of London A* **461**: 1685-1710.

[10] Huang Z. Y., Lü C. F., Chen W. Q., 2008, Benchmark solutions for functionally graded thick plates resting on Winkler–Pasternak elastic foundations, *Composite Structures* **85**(2): 95-104.

[11] Valter B., Ram M.K., Nicolini C., 2002, Synthesis of multiwalled carbon nanotubes and poly (o-anisidine) nanocomposite material: Fabrication and characterization of its Langmuir-Schaefer films, *Langmuir* **18**(5):1535-1541.

[12] Jafari Mehrabadi S., Sobhani Aragh B., Khoshkhahesh V., Taherpour A., 2012, Mechanical buckling of nanocomposite rectangular plate reinforced by aligned and straight single-walled carbon nanotubes, *Composites Part B-Engineering* **43**(4): 2031-2040.

[13] Malekzadeh P., Shojaee M., 2013, Buckling analysis of quadrilateral laminated plates with carbon nanotubes reinforced composite layers, *Thin-Walled Structures* **71**: 108-118.

[14] Shen H. S., 2009, Nonlinear bending of functionally graded carbon nanotube-reinforced composite plates in thermal environments, *Composite Structures* **91**(1): 9-19.

[15] Zhu P., Lei Z. X., Liew K. M., 2012, Static and free vibration analyses of carbon nanotube-reinforced composite plates using finite element method with first order shear deformation plate theory, *Composite Structures* **94**(4): 1450-1460.

[16] Sobhani Aragh B., Nasrollah Barati A.H., Hedayati H., 2012, Eshelby–Mori–Tanaka approach for vibrational behavior of continuously graded carbon nanotube-reinforced cylindrical panels, *Composites Part B-Engineering* **43**(4): 1943-1954.

[17] Alibeigloo A., Liew K.M., 2013, Thermoelastic analysis of functionally graded carbon nanotube-reinforced composite plate using theory of elasticity, *Composite Structures* **106**: 873-881.
[18] Moradi-Dastjerdi R., Foroutan M., Pourasghar A., Sotoudeh-Bahreini R., 2013, Static analysis of functionally graded carbon nanotube-reinforced composite cylinders by a mesh-free method, *Journal of Reinforced Plastic and Composites* **32**(9): 593-601.
[19] Lei Z. X., Liew K. M., Yu J. L., 2013, Large deflection analysis of functionally graded carbon nanotube-reinforced composite plates by the element-free kp-Ritz method, *Computational Methods in Applied Mechanics and Engineering* **256**: 189-199.
[20] Lei X. Z., Liew K. M., Yu J. L., 2013, Buckling analysis of functionally graded carbon nanotube-reinforced composite plates using the element-free kp-Ritz method, *Composite Structures* **98**: 160-168.
[21] Shen H. S., Xiang Y., 2014, Nonlinear vibration of nanotube-reinforced composite cylindrical panels resting on elastic foundations in thermal environments, *Composite Structures* **111**: 291-300.
[22] Lam K. Y., Wang C. M., He X. Q., 2000, Canonical exact solutions for Levy-plates on two-parameter foundation using Green's functions, *Engineering Structures* **22**: 364-378.
[23] Han J.B., Liew K.M., 1997, Numerical differential quadrature method for Reissner/Mindlin plates on two-parameter foundations, *International Journal of Mechanical Sciences* **39**(9): 977-989.
[24] Winkler E., 1867, *Die Lehre von der Elasticitaet und Festigkeit*, Prag, Dominicus.
[25] Pasternak P. L., 1954, On a new method of analysis of an elastic foundation by means of two foundation constants , *Gosudarstvennoe Izdatelstro Liberaturi po Stroitelstvui Arkhitekture*, Moscow.
[26] Huang Z.Y., Lü C.F., Chen W.Q., 2008, Benchmark solutions for functionally graded thick plates resting on Winkler–Pasternak elastic foundations, *Composite Structures* **85**(2): 95-104.
[27] Zhang D. G., 2013, Nonlinear bending analysis of FGM rectangular plates with various supported boundaries resting on two-parameter elastic foundations, *Archive of Applied Mechanics* **84**(1): 1-20.
[28] Shen S. H., Wang H., 2014, Nonlinear vibration of shear deformable FGM cylindrical panels resting on elastic foundations in thermal environments, *Composites Part B: Engineering* **60**: 167-177.
[29] Singha M. K., Prakash T., Ganapathi M., 2011, Finite element analysis of functionally graded plates under transverse load, *Finite Element in Analysis and Design* **47**(4): 453-460.
[30] Belytschko T., Lu Y.Y., Gu L., 1994, Element-free Galerkin methods, *International Journal of Numerical Methods in Engineering* **37**: 229-256.
[31] Zhu T., Atluri N.,1998, A modified collocation method and a penalty function for enforcing the essential boundary conditions in the element free Galerkin method, *Computational Mechanics* **21**: 211-222.
[32] Chen J.S., Chunhui P., Wu C.T., Liu W.K., 1996, Reproducing kernel particle method for large deformation of nonlinear structures, *Computational Methods Applied Mechanics and Engineering* **139**: 195-227.
[33] Memar Ardestani M., Soltani B., Shams Sh., 2014, Analysis of functionally graded stiffened plates based on FSDT utilizing reproducing kernel particle method, *Composite Structures* **112**: 231-240.
[34] Malekzadeh P., Golbahar Haghighi M. R., Alibeygi Beni A., 2011, Buckling analysis of functionally graded arbitrary straight-sided quadrilateral plates on elastic foundations, *Meccanica* **47**(2): 321-333.
[35] Shen H. S., Zhang C. L. , 2010, Thermal buckling and postbuckling behavior of functionally graded carbon nanotube-reinforced composite plates, *Materials & Design* **3**(7): 3403-3411.